www.czasopisma.pan.pl PAN POLSKA AKADEMIA NAUK www.journals.pan.pl

A R C H I V E S O F M E T A L L U R G Y A N D M A T E R I A L S

Volume 58 2013 Issue 2

DOI: 10.2478/amm-2013-0022

K. BRYŁA*, J. DUTKIEWICZ**, L.L. ROKHLIN***, L. LITYŃSKA-DOBRZYŃSKA**, K. MROCZKA*, P. KURTYKA*

MICROSTRUCTURE AND MECHANICAL PROPERTIES OF Mg-2.5%Tb-0.78%Sm ALLOY AFTER ECAP AND AGEING

MIKROSTRUKTURA I WŁAŚCIWOŚCI MECHANICZNE STOPU Mg-2.5%Tb-0.78%Sm PO PROCESIE ECAP I STARZENIU

The influence of ageing and Equal Channel Angular Pressing (ECAP) on the microstructure and mechanical properties of Mg-2.5%Tb-0.78%Sm alloy has been examined. The microhardness changes during ageing at 200°C show a slight increase. The aged microstructure at maximum hardness contains Mg_{12}(Tb,Sm) – metastable β' phase of size about 2-10 nm as dispersed precipitates. The orientation relationship between β' phase and the matrix was found as follows: $(0001)_{Mg} \parallel \left(1\bar{1}0\right)_{\beta'}$, $\left[2\bar{1}\bar{1}0\right]_{Mg} \parallel [116]_{\beta'}$. The ECAP passes were performed by two procedures: "I" – four passes at 350°C; "II" – one pass at 370°C, second pass at 340°C and third pass at 310°C. The grain size was reduced about 200 times as a results of ECAP process according "I" and "II" procedure. The grain refinement by ECAP improves significantly the compression yield strength and hardness. The Hall-Petch relationship was confirmed basing on microhardness measurements and the grain size after ECAP. The $Mg_{24}(Tb,Sm)_5$ and $Mg_{41}(Sm,Tb)_5$ particles smaller than 150 nm are located mainly at grain and subgrain boundaries and they prevent grain growth during ECAP processing. The microstructure evolution during ECAP can be described as dynamic recovery and continuous and discontinuous dynamic recrystallization.

Keywords: magnesium alloys with rare earth metals, ECAP, microstructure, ageing, mechanical properties

W pracy przeprowadzono badania mikrostruktury i właściwości mechanicznych stopu Mg-2,5%Tb-0,78%Sm po procesie starzenia oraz po odkształceniu plastycznym metodą ECAP. Starzenie stopu w temperaturze 200°C powoduje niewielki wzrost mikrotwardości. Mikrostruktura stopu starzonego o maksymalnej wartości twardości zawiera metastabilne drobnodyspersyjne wydzielenia Mg_{12}(Tb,Sm) – β' o wielkości 2-10 nm. Roztwór stały α-Mg wykazuje następujące zależności krystalograficzne z wydzielonymi cząstkami β': $(0001)_{\alpha Mg} \parallel \left(1\bar{1}0\right)_{\beta'}$, $\left[2\bar{1}\bar{1}0\right]_{\alpha Mg} \parallel [116]_{\beta'}$. Odkształcenie plastyczne metodą ECAP przeprowadzono stosując dwie procedury: „I" – cztery przejścia w 350°C, „II" – pierwsze w 370°C, drugie w 340°C i trzecie przejście w 310°C. Po procesie ECAP, dla obu procedur, nastąpiło dwustukrotne zmniejszenie wielkości ziarna. Zmniejszenie wielkości ziarna uzyskane metodą ECAP znacząco poprawia twardość oraz granicę plastyczności przy ściskaniu. Stwierdzono zależność Halla-Petcha pomiędzy wartościami mikrotwardości oraz wielkości ziaren uzyskanymi w wyniku odkształcenia metodą ECAP. Cząstki $Mg_{24}(Tb,Sm)_5$ i $Mg_{41}(Sm,Tb)_5$ mniejsze niż 150 nm wydzielone na granicach ziaren i podziaren zapobiegają ich wzrostowi podczas procesu ECAP. Zmiany mikrostruktury zachodzące podczas procesu ECAP można opisać procesami dynamicznego zdrowienia oraz dynamicznej rekrystalizacji.

1. Introduction

The research and development of magnesium alloys have expanded tremendously for a new practical applications during the past decade, among others in the automotive industry, portable electronics and medical devices. Currently, there is a growing interest in developing new applications in the defense and aerospace industries [1]. The main limitation for a wider use of magnesium alloys components are, inter alia: poor high temperature strength, formability and limited ductility at ambient temperature.

New magnesium alloys with rare earth elements additions appears promising in improving the mechanical performance at room and elevated temperature and corrosion resistance. For example, the Mg-1.8Gd-1.8Y-0.7Zn-0.2Zr (at.%) alloy produced by hot extrusion has an impressive strength of over 470 MPa and elongation to failure of 8% [2].

Magnesium alloys containing individual rare earth metals have an improved strength properties due to precipitation strengthening, both at ambient and elevated temperatures as compared to the commercial alloys [3,4]. As evidenced by earlier research [5], the ternary Mg-Sm-Tb system offers the possibility of decomposition of Mg-based solid solution causing the strengthening effect.

The grain size refinement generally results in a significant improvement in mechanical properties according to the Hall-Petch equation and the equal channel angular pressing (ECAP) is one of the method to obtain ultrafine grain metal-

* INSTITUTE OF TECHNOLOGY, PEDAGOGICAL UNIVERSITY OF CRACOW, 2 PODCHORĄŻYCH STR., 30-084 KRAKÓW, POLAND
** INSTITUTE OF METALLURGY AND MATERIAL SCIENCE, POLISH ACADEMY OF SCIENCES, 25 W. REYMONTA STR., 30-059 KRAKÓW, POLAND
*** BAIKOV INSTITUTE OF METALLURGY AND MATERIAL SCIENCE, RUSSIAN ACADEMY OF SCIENCES, 49, LENINSKY PROSPECT, 119991 GSP-1, MOSCOW, RUSSIA

lic materials [6]. Previous studies have shown that ultra-fine grained steels, aluminum and copper alloys, as well as composites fabricated by ECAP exhibit an improved ductility, strength and superplasticity [7-10]. Even more difficult is to process magnesium alloys, due to their hexagonal close-packed structure, however it was successfully demonstrated in strength improvements and grain refinement [11].

The purpose of this study is to investigate the microstructure and mechanical properties of Mg-2.5%Tb-0.78%Sm alloy after ECAP carried out with two different procedures. In addition, the effect of aging treatment on the microstructure and mechanical properties was examined.

2. Experimental procedures

The magnesium alloy containing 2.52% Tb and 0.78% Sm was prepared in an electrical resistance furnace by casting in steel crucible under a protective flux consisting chlorides and fluorides of the alkali and alkali-earth metals. The as-cast ingot in diameter of 30 mm was homogenized at 500°C for 6 hours and rolled at 450°C down to the thickness of 10 mm. An ingot was cut into billets with dimensions 10×10×50 mm and then subjected to ECAP processing. The square billets were pressed through the ECAP facility with 90° intersecting channels at speed of 10 mm/min using a hydraulic press machine. The ECAP die used in experiments was earlier described in detail [12]. The effective strain in a single pass through the die is close to 1. Samples were coated with graphite paste to assure lubrication during pressing before inserting in ECAP facility channel. For each pass, ECAP facility was heated up to right temperature and a sample was held in die channel for 10 minutes to reach the temperature stabilization. The temperature was measured by a thermocouple near the channel wall with accuracy to ±5°C. The ECAP passes were performed by two procedures following B_C route at the elevated temperature: "I" – four passes at 350°C; "II" – one pass at 370°C, second pass at 340°C and the third pass at 310°C. A second procedure was done to prevent the temperature induced recrystallization processes and grain growth during ECAP passes.

For microstructural examinations and mechanical testing, the specimens were cut from the middle of sample along the plane parallel to the extrusion direction [12].

The Mg-2.52%Tb-0.78%Sm alloy after rolling was aged at 200°C after solution treatment at 525°C for 2 hours and water quenching. Microhardness (HV0.1) measurements and high resolution transmission electron microscopy (HRTEM) were carried out to evaluate the effect of precipitation hardening on microstructure and mechanical properties.

The microstructure was studied using an optical microscopy and an average grain size was calculated by the method of secants. The samples were prepared for optical metallography using standard metallographic procedures and were etched in a solution of 1 ml acetic acid, 4.2 g picric acid, 10 ml H_2O and 75 ml ethanol. Thin foils were prepared by electropolishing in a solution of 80% perchloric acid and 20% ethanol at -50°C, and studied by means of Tecnai G2 F20 transmission electron microscopy (TEM).

The compressive tests and Vickers microhardness measurements were performed before and after ECAP. The compressive tests of specimens of cylindrical shape with diameter of 4 mm and height of 6 mm from the billets were carried out at the strain rate $1.8\times10^{-3}s^{-1}$. Vickers microhardness measurements of investigated samples were determined at the load of 100 g for 10 s.

3. Results and discussion

3.1. Microstructure

The microstructure of as-cast Mg-2.5%Tb-0.78%Sm alloy consisted of typical magnesium rich dendrite structure with inhomogeneous grain size distribution of an average grain size of about 550 μm (Fig. 1a). The microsegregation of Tb and Sm, and precipitates was observed between dendrites and at the grain boundaries (Fig. 1b). This enrichment is shown in SEM image in backscattered mode with an EDS line scan analysis performed across the microsegregation (Fig. 1c).

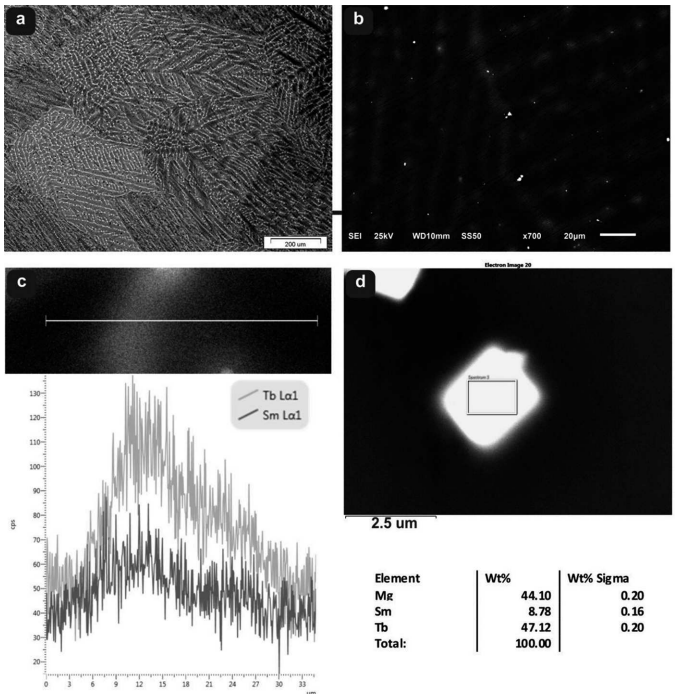

Fig. 1. The microstructure of the as-cast Mg-2.5%Tb-0.78%Sm alloy: (a) grain and dendrite microstructure (OM), (b) microsegregation of Tb and Sm at grain boundaries and between dendrites (SEM), (c) SEM image in backscattered mode with an EDS line-scan performed across microsegregation, (d) $Mg_{24}(Tb,Sm)_5$ particle and its chemical composition determined by SEM/EDS

The main particles observed in α-Mg solid solution matrix were cuboid-shaped $Mg_{24}(Tb,Sm)_5$ compounds with a diagonal size of between 0.5-5 μm, distributed at the grain boundaries and between dendrites (Fig. 1d). The irregular-shaped $Mg_{41}(Tb,Sm)_5$ precipitates with a size of about 1-3 μm were rarely observed. The clusters of precipitates, mainly $Mg_{24}(Tb,Sm)_5$, close to the grain boundaries were also observed. The precipitated phases found in the alloy correspond to the binary Mg-Tb and Mg-Sm phase diagrams.

The as-cast alloy was homogenized at 500°C for 6 hours and then hot rolled at 450°C and subsequently subjected to ageing and ECAP processing. The microstructure of the

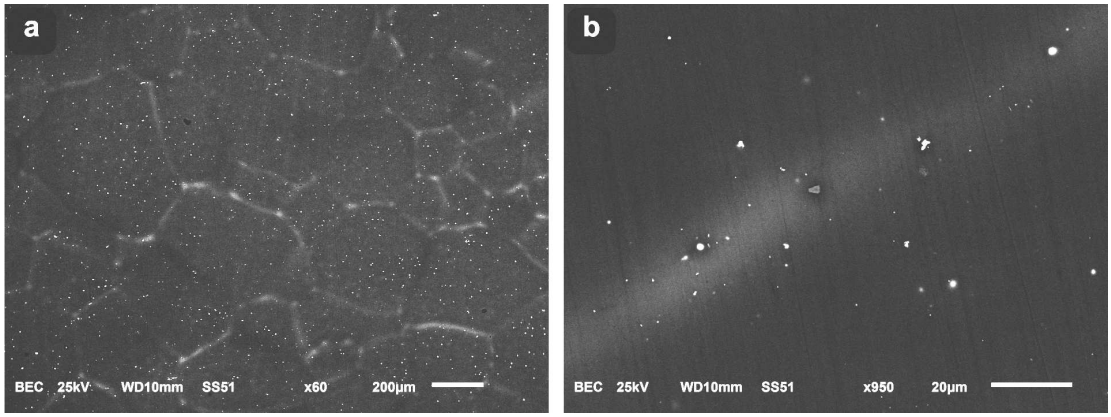

Fig. 2. The microstructure of the as-rolled Mg-2.5%Tb-0.78%Sm alloy at 450°C: (a) grain structure (SEM), (b) precipitates at and within the grain boundaries (SEM)

as-rolled material shows of heterogeneously distributed deformed grains (Fig. 2a and 3a). The average grain size of the specimen after hot rolling was about 250 μm and the precipitates, mainly $Mg_{24}(Tb,Sm)_5$, were located at and within the grain boundaries (Fig. 2b).

The hot rolled ingot was cut into billets and subjected to ECAP processing. The attempts of performing ECAP procedure at lower temperature than 350°C were unsuccessful, due to cracks formation. The grain structure development of Mg-2,5%Tb-0,78%Sm alloy deformed in ECAP die is shown in Figure 3. After single pass at 350°C, a large fraction of the grains are elongated in the direction of ECAP pressing and the microstructure was characterized by bimodal distribution of fine grains of 1-5 μm and larger grains of 15-20 μm.

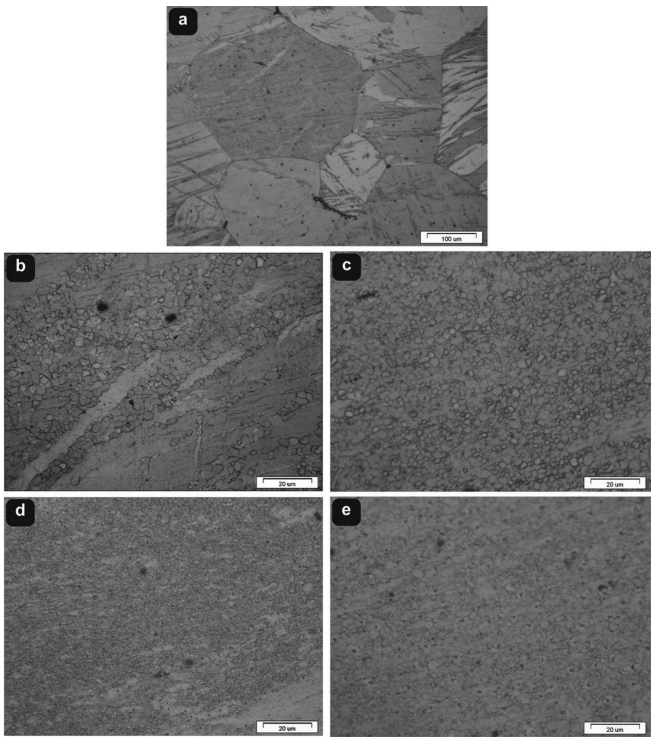

Fig. 3. The grain structure development of the Mg-2.5%Tb-0.78%Sm alloy during ECAP: (a) as rolled at 450°C – the initial structural state of the billets before ECAP, (b) after single pass at 350°C, (c) after one pass at 370°C and second at 340°C, (d) after one pass at 370°C, second at 340°C and third at 370°C – "II" procedure, (e) after four passes at 350°C – "I" procedure

The bimodal grain structure has been already observed during ECAP of AZ31 and ZK60 magnesium alloys [6,11,12]. It was explained by the fact that only favorable oriented grains were deformed and refined as first during ECAP and larger less deformed grains remained in the microstructure. However, the dynamic recrystallization cannot be neglected in this process. Experiments show that a homogenous grain structure may be achieved after one pass of ECAP when using an alloy with an initial fine microstructure.

A heterogeneous grain structure was observed after processing an alloy having an initial coarse-grained structure. A summary of the average grain size evolution of the Mg-2.5%Tb-0.78%Sm alloy after ECAP is shown in Table 1.

TABLE 1
Average grain size of the Mg-2.5%Tb-0.78%Sm alloy after ECAP in μm

	Initial: as-rolled	**ECAP**		**(B)**	**(A)**
		1 pass	**2 passes**	**3 passes**	**4 passes**
Temperature	450°C	350°C	370°C =>340°C	370°C =>340°C =>310°C	350°C
Average grain size	249.3	12.6	2.7	1.5	1.3
Standard deviation	99.1	8.2	4.9	2.2	0.8

The coarse-grain fraction decreases with the number of ECAP passes and after 4 passes at 350°C the homogeneity in grain size distribution was obtained with the average grain size of 1.3 μm. A significant reduction in grain size was also observed after 2 and 3 passes with decreasing the ECAP temperature at each successive pass. The grain refinement according to the "II" procedure was obtained down to 1.5 μm. Nevertheless, there were still some areas with coarsened grains.

TEM studies have revealed a strongly deformed microstructure of the Mg-2.5%Tb-0.78%Sm alloy after single pass of ECAP at 350°C (Fig. 4). The stored energy due to an increase of dislocation density and other defects is a driving

force for recovery, dynamic recrystallization and grain growth to lower the overall energy of the system.

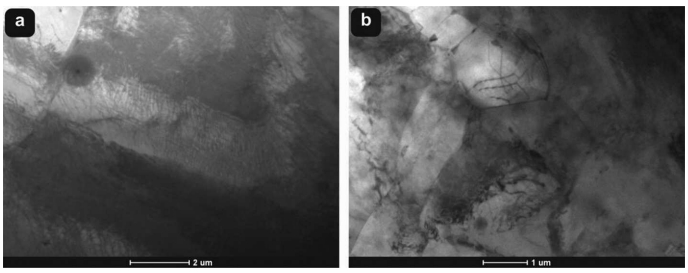

Fig. 4. TEM micrographs of the Mg-2.5%Tb-0.78%Sm alloy after single pass of ECAP at 350°C: (a) areas with coarse grains, (b) the areas with fine grains

A high dislocation density and several parallel groups of elongated subgrains were visible, especially in the coarse-grained areas (Fig. 4a). The dislocation rearrangements into cells and walls, and the formation of subgrain boundaries also in the fine grains were observed (Fig. 4b). The fraction of fine grains increases with an increasing number of ECAP passes, but the grain microstructure remained heterogeneous and consisted of coarse and fine grains. Figure 5a shows the microstructure of investigated alloy after 3 ECAP passes (according to "II" procedure) and the evidence of shear bands separating grains indicated by dotted line in the micrograph. Fine grains or subgrains in the vicinity shear bands and the rearrangement of the stored dislocations to form subgrain boundaries were observed. The findings of previous studies on ECAP processing of AZ31 magnesium alloy demonstrates that nucleation of new grains occurred mainly within the shear zones and along grain boundaries together with rearrangements of dislocations to form subgrain structures, leading to a gradual formation of new grain boundaries as suggested also in [13]. The ring-like selected area diffraction pattern can be indexed as h.p.c. structure of α-Mg, as shown in Fig. 5.b. It indicates that a large number of small grains are present in the microstructure, probably resulting from recovery and recrystallization within the shear bands.

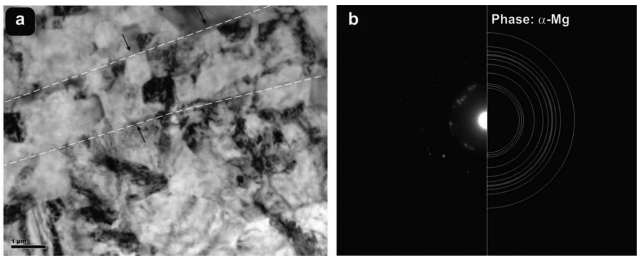

Fig. 5. TEM micrographs of the Mg-2.5%Tb-0.78%Sm after 3 passes according to the "II" procedure: (a) the bright-field image of grain and subgrain structure with visible shear bands (indicated by dotted line), (d) ring-like diffraction pattern of α-Mg

$Mg_{24}(Tb,Sm)_5$ cuboid-shaped particles smaller than 150 nm were revealed in the scanning-TEM mode (STEM) and identified by an Energy Dispersive Spectra (EDS) analysis (Fig. 6). These precipitates are located mainly at grain boundaries and they prevent grain growth during ECAP processing. The $Mg_{24}(Tb,Sm)_5$ compounds precipitates also at the subgrain boundaries and the smaller particles probably form during deformation by ECAP. Besides the above-mentioned compounds the small amount of oval-shaped $Mg_{41}(Tb,Sm)_5$ precipitates can be found. A high dislocation density was observed in many grains and subgrains, and some other grains were mostly of dislocation-free.

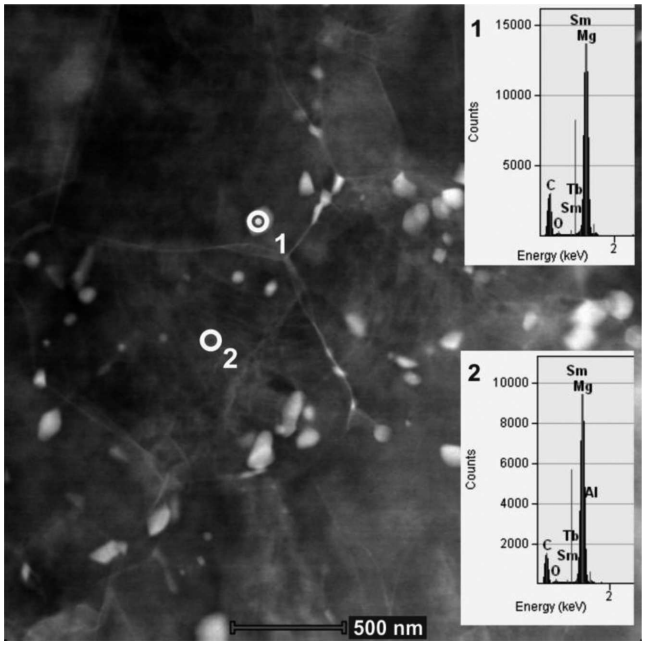

Fig. 6. The microstructure of the Mg-2.5%Tb-0.78%Sm alloy after 3 passes of ECAP with according with "II" procedure: High Angle Annular Dark Field (HAADF) image and Energy Dispersive spectra (EDS) spot analysis of the matrix and particle (points 1 and 2)

After 4 passes of ECAP at 350°C, the grain microstructure was more homogenous in comparison to sample after 3 passes with according to the "II" procedure (see Fig. 3e). An additional ECAP pass results in heavy straining in the large grains and it promotes the dynamic recrystallization and hence the grain size reduction. The dynamic recrystallization take place preferably at sites were the dislocation density is high. The microstructure with a high dislocation density within grains and formation of subgrains from dislocation cell walls was observed. A few recrystallized grains and the presence of dislocation within these grains probably induced by large strains by ECAP can be seen. The precipitates were located mainly at grain and sub-boundaries. In Figure 7, a large $Mg_{24}(Tb,Sm)_5$ cuboid-shaped particle of about 500 nm on the grain boundary was indentified. However, there were also precipitate-free zones along grain boundaries (Fig. 7b).

The current microstructural study shows that the grain refinement is a complex process which proceeds continuously with an increasing strain during ECAP passes. The mechanism of the grain refinement can be attributed to the combination of mechanical shearing and thermally activated processes like dynamic recovery and recrystallization where the driving force is strain imposed in processing by ECAP.

The microstructure of the Mg-2.5%Tb-0.78%Sm alloy after ECAP deformation in a all samples was metastable and consisted of a high density of dislocation heterogeneously distributed within grains. The dislocations arranged themselves into walls and subgrains were formed. The stored energy in the material during plastic deformation by ECAP can induce

the discontinuous dynamic recrystallization (DDRX), which is characterized by nucleation and grain growth and the continuous dynamic recrystallization (CDRX), which is proceeded by the progressive accumulation of dislocations in low angle boundaries, leading to an increase of their misorientation and the formation of high angle boundaries. The TEM study of the Mg-2.5%Tb-0.78%Sm alloy have revealed only a small amount of new recrystallized grains at the shear bands and in the area along grain boundaries, therefore it suggests DDRX. It was reported in [13,14] that DDRX occurs in AZ31 alloy during ECAP passes coursing refinement of the grain structure. On the other hand, another studies have shown that CDRX took place during ECAP of the same alloy [15,16]. CDRX was earlier observed in deformation of coarse-grained Al [17] and in superplastic deformation of TiAl alloy [18], which was controlled by dislocation slip and climb. DDRX processes probably dominate during the grain refinement of the alloy by ECAP. To identify a continuous dynamic recrystallization process, the misorientation angles of subgrain and grain boundaries measurements should be done after ECAP passes.

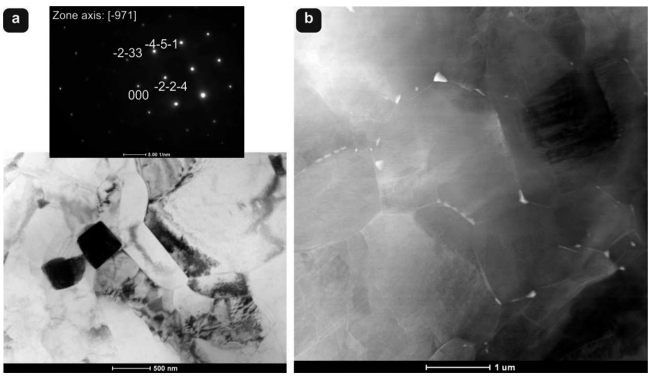

Fig. 7. The microstructure of the Mg-2.5%Tb-0.78%Sm alloy after 4 passes of ECAP at 350°C (with according to "I" procedure): (a) the TEM bright-field image of grain structure and SADP of the $M_{24}(Tb,Sm)_5$ particle, (b) STEM HAADF image

3.2. Aging

The solubility of samarium and terbium in the solid magnesium is limited and decreases with lowering temperature with according to the phase equilibrium systems: Mg-Tb and Mg-Sm [5]. It provides the possibility of precipitation hardening. Previous studies [19,20] have shown that the binary alloys of Mg-Sm and Mg-Tb system with 2-4% Sm and >10%Tb after aging treatment have the high strength characteristics at room and at elevated temperature. The present investigations were performed on magnesium alloy with 2.52%Tb and 0.78% Sm in order to allow deformation during ECAP passes.

The as-rolled Mg-2.52%Tb-0.78%Sm alloy was aged at 200°C after solution treatment at 525°C for 2 hours and water quenching. The microhardness peak after 45 minutes of aging at 200°C reached about of 67 (Fig. 8). As expected, only a slight increase in Vickers-microhardness was noticed, because the content of Tb and Sm was less than their maximum solubility in solid magnesium.

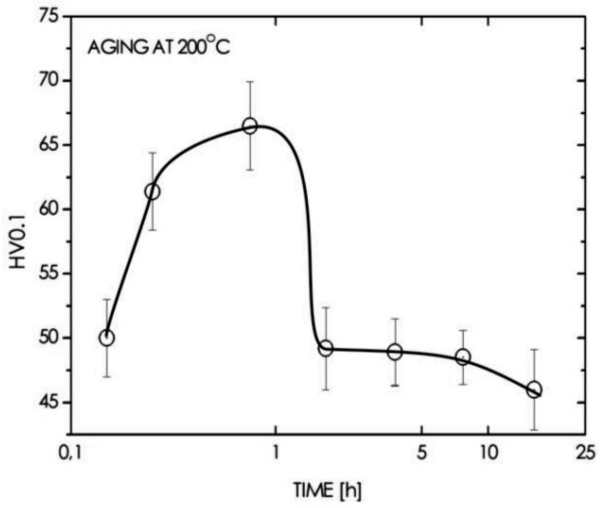

Fig. 8. The Vickers micro-hardness changes of as-rolled Mg-2.52%Tb-0.78%Sm alloy during ageing at 200°C after solution treatment at 525°C for 2 hours

The microstructure of precipitation-hardened alloy contained of fine spheroidal-shaped precipitates with a size about of 2-10 nm (Fig. 9a). The chemical analysis of precipitates in microstructure indicates the presence of $Mg_{12}(Tb,Sm)$ phase – metastable β' [Fig. 9b], which had been previously observed in aged WE43, WE54 and Mg-xY-1.5LPC-0.4Zr alloy [21,22]. The β' phase has a base-cantered orthorhombic structure. A high resolution TEM image of β' phase in the magnesium matrix with fast Fourier Transform (FFT) present in Figure 10. The orientation relationship between β' phase and the matrix can be stated as follows: $(0001)_{Mg} \parallel \left(1\bar{1}0\right)_{\beta'}$, $\left[2\bar{1}10\right]_{Mg} \parallel [116]_{\beta'}$.

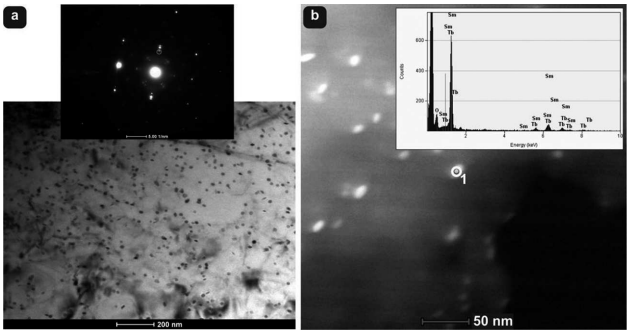

Fig. 9. The microstructure of precipitation-hardened Mg-2.52%Tb-0.78%Sm alloy: (a) fine spheroidal-shaped precipitates with corresponding SADP, (b) STEM mode image with an EDS spot analysis of β' phase particle: 93.5% Mg, 4.7% Tb, 1.8% Sm (in atomic %)

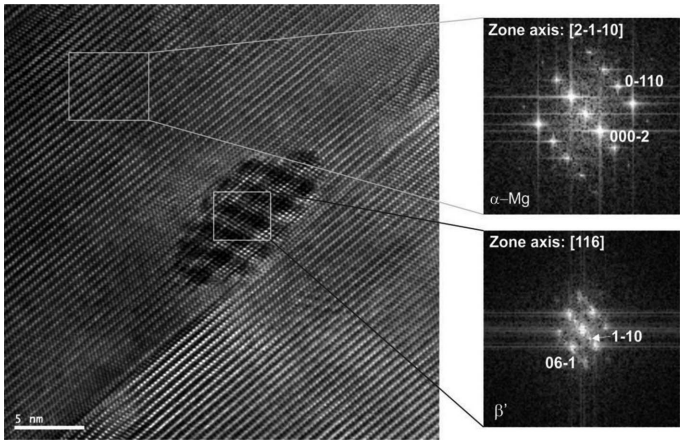

Fig. 10. β' phase in precipitation-hardened Mg-2.52%Tb-0.78%Sm alloy: HRTEM image and FFT image from areas where α-Mg and β' phase exist

3.3. Mechanical properties

The strengthening effect caused by a decrease in the grain size of alloy is processed by ECAP. The Hall-Petch relationship based on the Vickers micro-hardness was observed for the deformed samples (Fig. 11a). This trend for other magnesium alloys deformed by ECAP was also reported in [12,16]. The Vickers microhardness value after only the first pass was higher than in age-hardened sample. Results for the ECAP-deformed samples according to "I" and "II" procedures were similar (about 80 HV).

The compression tests at ambient temperature were performed for the samples in as-cast condition, age-hardened and in deformed state – after ECAP. The deformation curves were plotted as the true stress versus the true strain (Fig. 11b). For the as-cast sample, the compressive yield strength was about 65 MPa. The ECAP pressing resulted in a significant increase of the compressive yield strength of about 185 MPa for both samples deformed according "I" and "II" procedure. However, the alloy after 4 passes at 350°C ("I" procedure) had a higher value of the compressive strength of about 310 MPa, which can be attributed to a more homogeneous grain structure due to additional pass through the ECAP die. Two times higher compressive yield strength was achieved already after only single ECAP past, as compared to as cast. The age-hardened alloy had a compressive yield strength of 67 MPa, similarly to as-cast condition, but the compressive strength was about 20 MPa higher. These results show that the grain refinement by ECAP improves significantly the mechanical properties of the Mg-2.52%Tb-0.78%Sm alloy at room temperature.

4. Conclusions

The microstructure of the as-cast Mg-2.52%Tb-0.78%Sm alloy consists of a typical magnesium rich dendrite structure. The microsegregation of Tb and Sm, $Mg_{24}(Tb,Sm)_5$ and $Mg_{41}(Sm,Tb)_5$ precipitates was observed between dendrites.

The Vickers micro-hardness studies of as-rolled alloy during ageing show a slight increase after 45 minutes at 200°C. The aged microstructure at maximum hardness contains metastable β' phase $Mg_{12}(Tb,Sm)$ as dispersed precipitates. The orientation relationship between phase and the matrix can be stated as follows: $(0001)_{Mg} \parallel \left(1\bar{1}0\right)_{\beta'}$, $\left[2\bar{1}\bar{1}0\right]_{Mg} \parallel [116]_{\beta'}$.

The grain size is reduced about 200 times as results of ECAP process according "I" and "II" procedure. The grain refinement by ECAP improves significantly the compression yield strength and hardness. The Hall-Petch relationship was confirmed between the Vickers microhardness and the grain size changes achieved by ECAP. The maximum value of the compressive yield strength is similar to both procedures, and is about 185 MPa, which is about 3 times higher as compared to the as-cast condition.

The microstructure of Mg-2.52%Tb-0.78%Sm alloy after a single ECAP pass consists of typical bimodal structure. The presence of high dislocation density was observed in most of grains. The $Mg_{24}(Tb,Sm)_5$ and $Mg_{41}(Sm,Tb)_5$ particles smaller than 150 nm are located mainly at grain and subgrain boundaries and they prevent grain growth during ECAP

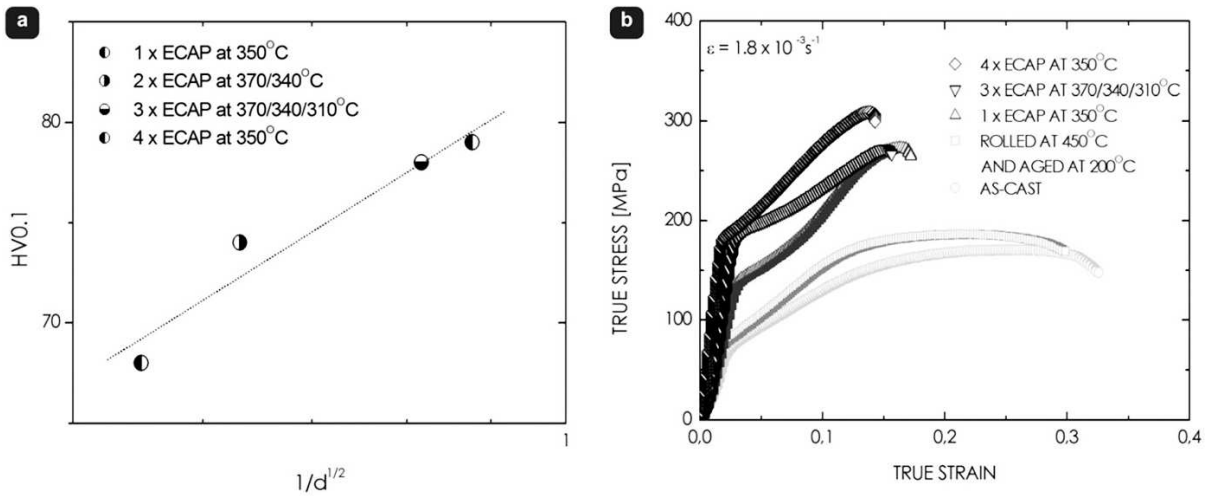

Fig. 11. Mechanical properties of Mg-2.52%Tb-0.78%Sm alloy: (a) Hall-Petch relationship for the ECAP deformed samples, (b) compression true stress versus true strain at room temperature of the as-cast, age-hardened and ECAP-ed samples

processing. The microstructure evolution during ECAP results from recovery and continuous and discontinuous dynamic recrystallization. After 4 passes according "II" procedure, a microstructure is more homogenous than after 3 passes according "I" procedure, which contains of very fine, but also coarsened grains.

REFERENCES

[1] S.R. Agnew, J.F. Nie, Preface to the viewpoint set on: The current state of magnesium alloy science and technology, Scripta Materialia **63**, 671-673 (2010).

[2] T. Homma, N. Kunito, S. Kamado, Fabrication of extraordinary high-strength magnesium alloy by hot extrusion, Scripta Materialia **61** (6), 644-647 (2009).

[3] L.L. Rokhlin, The regularities in the Mg-Rich Parts of the Phase Diagrams, Phase Transformations and Mechanical Properties of Magnesium Alloys with Individual Rare Earth Metals, Archives of Metallurgy and Materials **52** (1), 5-11 (2007).

[4] L.L. Rokhlin, T.V. Dobatkina, N.I. Nikitina, V.N. Timofeev, I.E. Tarytina, Effect of Cerium on the Kinetics of Decomposition of Supersaturated Solid Solution in Mg-Y Alloys, Physics of Metals and Metallurgy **100** (2), 160-164 (2005).

[5] L.L. Rokhlin, T.V. Dobatkina, E.A. Luk'anova, I.G. Korolkova, A.S. Polikanova, Phase Equilibria in Solid Mg-Rich Mg-Sm-Tb Alloys, Metally **4**, 99-106 (2010).

[6] R.Z. Valiev, T.G. Langdon, Principles of equal-channel angular pressing as a processing tool for grain re?nement, Progress in Materials Science **51**, 881-981 (2006).

[7] J. Kusnierz, J. Bogucka, Effect of ECAP processing on the properties of cold rolled copper, Archives of Metallurgy, Archives of Metallurgy **48**, 173 (2003).

[8] H. Paul, T. Baudin, F. Brisset, Effect of strain path and second phase particles on microstructure and texture evolution of AA3104 aluminum alloy processed by ECAP, Archives of Metallurgy and Materials **56**, 245-261 (2011).

[9] M. Greger, R. Kocich, L. Čížek, L.A. Dobrzański, M. Widomská, Influence of ECAP technology on the metal structures and properties, Archives of Materials Science and Engineering **28** (12), 709-716 (2007).

[10] L. Bian, W. Liang, G. Xie, W. Zhang, J. Xue, Enhanced ductility in an Al-Mg2Si in situ composite processed by ECAP using a modified B_C route, Materials Science and Engineering: A **528** (9), 3463-3467 (2011).

[11] R.B. Figueiredo, T.G. Langdon, Achieving Microstructural Refinement in Magnesium Alloys through Severe Plastic Deformation, Materials Transactions **50**, 01, 111-116 (2009).

[12] K. Bryła, J. Dutkiewicz, L. Lityńska-Dobrzyńska, L.L. Rokhlin, P. Kurtyka, Influence of number of ECAP passes on microstructure and mechanical properties of AZ31 magnesium alloy, Archives of Metallurgy and Materials **57** (3), 711-717 (2012).

[13] C.W. Su, L. Lu, M.O. Lai, A model for grain refinement mechanism in equal channel angular pressing of Mg alloy from microstructural studies, Material Science and Engineering **A 434**, 227-236 (2006).

[14] M. Janeček, M. Popov, M.G. Krieger, R.J. Hellmig, Y. Estrin, Mechanical properties and microstructure of a Mg alloy AZ31 prepared by equal channel angular pressing, Materials Science and Engineering **A462**, 116-120 (2007).

[15] L. Jin, D. Lin, D. Mao, X. Zeng, B. Chen, W. Ding, Microstructure evolution of AZ31 Mg alloy during equal channel angular extrusion, Materials Science and Engineering **A 423**, 247-252 (2006).

[16] H.K. Kim, W.J. Kim, Microstructural instability and strength of an AZ31 Mg alloy after serve plastic deformation, Materials Science and Engineering **A385**, 300-308 (2004).

[17] C. Liu, S. Liang, X. Zhang, Continuous dynamic recrystallization and discontinuous dynamic recrystallization in 99.99% polycrystalline aluminum during hot compression, Transactions of Nonferrous Metals Society of China **15** (1), 82-86 (2005).

[18] D. Lin, F. Sun, Superplasticity in a large-grained TiAl alloy, Intermetallics **12** (7-9), 875-883 (2004).

[19] M.E. Drits, L.L. Rokhlin, N.P. Abrukina, Mechanical properties of binary alloys of the Mg-Sm system, Metal Science and Heat Treatment **27** (7), 508-510 (1985).

[20] M.E. Drits, L.L. Rokhlin, E.M. Padezhnova, L.S. Guzei, Phase diagram and mechanical properties of Mg-Tb alloys, Metal Science and Heat Treatment **20** (9), 771-774 (1978).

[21] J.F. Nie, B.C. Muddle, Characterisation of strengthening precipitate phases in a Mg-Y-Nd alloy, Acta Materialia **48**, 1691-1703 (2000).

[22] J. Wang, J. Nie, R. Wang, Y. Xu, X. Zhu, G. Ling, Effect of Y on the age hardening response and mechanical properties of Mg-xY-1.5LPC-0.4Zr alloys, Transactions of Nonferrous Metals Society of China **22** (1), 1549-1555 (2012).

Received: 20 January 2013.